

A study of  $K^*(890)$  and  $K^*(1420)$  production

mechanisms in  $K^+ p \rightarrow K^+ \pi^- \Delta^{++}$  at 13 GeV/c\*

P. Estabrooks\*\* and A. D. Martin  
Department of Physics,  
University of Durham,  
Durham City, England.

G. W. Brandenburg<sup>†</sup>, R. K. Carnegie<sup>††</sup>, R. J. Cashmore<sup>†††</sup>, M. Davier<sup>†</sup>,  
W. M. Dunwoodie, T. A. Lasinski, D. W. G. S. Leith, J. A. J. Matthews<sup>††</sup>,  
P. Walden<sup>†††</sup>, and S. H. Williams

Stanford Linear Accelerator Center  
Stanford University, Stanford, California 94305

Abstract

Amplitudes for  $K^*(890)$  and  $K^*(1420)$  production, and their lower spin background, are determined from an analysis of the  $K\pi$  angular distribution observed in  $K^+ p \rightarrow K^+ \pi^- \Delta^{++}$  at 13 GeV/c. The exchange mechanisms responsible for  $K^*\Delta$  production are studied, and a simple model is introduced which describes all features of the data.

(To be published in Nucl. Phys. B)

---

\*Work supported by the U.K. Science Research Council and the U.S. Energy Research and Development Administration.

Present address:

\*\* Department of Physics, McGill University, Montreal, Quebec, Canada.

† Department of Physics, MIT, Cambridge, Massachusetts.

†† Department of Physics, Carleton University, Ottawa, Ontario, Canada.

††† Department of Physics, Oxford University, Keble Road, Oxford, England.

† Laboratoire de l'Accélérateur Linéaire, Orsay, France.

†† Department of Physics, Michigan State University, East Lansing, Michigan.

††† TRIUMF, University of British Columbia, Vancouver, B.C., Canada.

## 1. Introduction

The high statistics data<sup>1)</sup> for  $K^+p \rightarrow K^+\pi^-\Delta^{++}$  at 13 GeV/c afford the opportunity of studying  $K^*(890)$  and  $K^*(1420)$  resonance production. For each resonance we use the observed  $K^+\pi^-$  angular distributions to determine the  $t$  structure of the  $K^*\Delta$  production amplitudes. Although a complete description of  $K^+p \rightarrow K^*\Delta^{++}$  requires twice as many amplitudes<sup>†</sup> as one of  $KN \rightarrow K^*N$ , the dominance of  $\pi$  exchange at small  $t$  allows us to simplify the problem, and to perform amplitude analyses in much the same way as for  $KN \rightarrow K^*N$ .<sup>3,4,5)</sup> In order to perform reliable amplitude analyses, we find that it is crucial to include the lower  $K\pi$  partial waves under the  $K^*$  resonances. Having obtained the amplitudes, we then describe their  $t$  structure in terms of a simple model based on  $\pi$ ,  $B$ ,  $\rho$  and  $A_2$  exchange, together with non-evasive or 'cut' contributions. This economical model is able to describe all features of the data in both the  $K^*(890)$  and the  $K^*(1420)$  mass regions. Consequently we can study the production mechanisms as a function of the produced  $K\pi$  mass.

Besides their intrinsic interest, a knowledge of the  $(K\pi)\Delta$  production mechanisms is important for the determination of  $K\pi$  partial waves by extrapolation to the  $\pi$  exchange pole. In particular, we can investigate whether the advantage of using the non-vanishing, non-flip  $\pi$  exchange in the  $Kp \rightarrow K\pi\Delta$  reaction (as compared to  $Kp \rightarrow K\pi n$ ) is offset by the relatively large values of  $|t_{\min}|$  that occur with increasing  $K\pi$  mass.

The plan of the paper is as follows. §2 and §3 are devoted to  $K^*(890)\Delta$  and  $K^*(1420)\Delta$  production respectively. In each section, the discussion proceeds from the less- to the more-model-dependent results. For example, for  $K^*(890)\Delta$  production we present first, in §2.1, the

---

<sup>†</sup>See, for example, ref. 2.

amplitude bounds that follow directly from the positivity of the  $K\pi$  density matrix. We then describe, in §2.2, an amplitude analysis of the  $K\pi$  angular distribution based on the minimum number of assumptions, and finally, in §2.3, we use an exchange model to generate the amplitude structure. Our summary and conclusions are contained in §4.

## 2. $K^*(890)$ production

In the mass region  $0.87 < M_{K\pi} < 0.92$  GeV, the  $K^+p \rightarrow (K^+\pi^-)\Delta^{++}$  reaction can be described by S and P wave  $K\pi$  spin states only. It is convenient to discuss the  $K\pi$  angular distribution in terms of the quantities†  $S_0, P_0, P_-$  and  $P_+$ , where  $S_0$  and  $P_0$  describe helicity zero  $K\pi$  production and, to leading order in energy,  $P_{\pm} \equiv (P_{\lambda=1} \pm P_{\lambda=-1})/\sqrt{2}$  describe helicity one production by natural and unnatural parity exchange respectively. Since, in this experiment<sup>1)</sup>, there is no information on baryon polarisation, each of the above amplitudes is an incoherent sum of four independent amplitudes, that is

$$|L_i|^2 \equiv \sum_{\Delta, N} |L_{\Delta N}^i|^2 \quad (1)$$

where  $(\Delta, N) \equiv (2\lambda_{\Delta}, 2\lambda_N) = (3+), (1+), (3-)$  and  $(1-)$ . The degree of (spin) coherence,  $\xi_{10}$ , between  $P_0$  and  $P_-$ , for example, is defined by

$$\vec{P}_- \cdot \vec{P}_0^* \equiv \sum_{\Delta, N} P_{\Delta N}^- P_{\Delta N}^{0*} \equiv \xi_{10} |P_0| |P_-| e^{i\phi_{10}} \quad (2)$$

where  $0 \leq \xi_{10} \leq 1$ , with analogous expressions for  $\vec{S}_0 \cdot \vec{P}_0^*$  and  $\vec{S}_0 \cdot \vec{P}_-^*$ . Before expressing the observables in terms of amplitudes, we note that in the

---

† These amplitudes may be regarded as vectors in the space spanned by the baryon helicity eigenstates.

$K^*(890)$  resonance region,  $\delta_p$ , the phase of the  $K\pi$  P wave, varies rapidly with  $M_{K\pi}$  while  $\delta_s$  is virtually independent of  $K\pi$  mass. The  $\delta_L$  are related to the  $I=\frac{1}{2}, \frac{3}{2}$  phase shifts by

$$\delta_L = \arg \left[ \sin \delta_L^1 e^{i\delta_L^1} + \frac{1}{2} \sin \delta_L^3 e^{i\delta_L^3} \right] \quad (3)$$

To allow for the different mass dependences of the S and P wave amplitudes we average the observable amplitude combinations over the  $K^*$  mass bin assuming that  $\delta_p^3=0$  and that  $\delta_p^1$  is given by a Breit-Wigner resonance form  $\left[ M(K^*) = 0.893 \text{ GeV}, \Gamma(K^*) = 0.05 \text{ GeV}, R = 5 \text{ GeV}^{-1} \text{ as in ref. 5.} \right]$  and that  $\delta_s$  and the production mechanisms are independent of  $M_{K\pi}$ . The observable moments of the  $K\pi$  angular distribution can then be written as:

$$\begin{aligned} \sigma \equiv \frac{d\sigma}{dt} &= |S_0|^2 + \langle \sin^2 \delta_p \rangle (|P_0|^2 + |P_+|^2 + |P_-|^2) \\ \sigma(\rho_{00}-\rho_{11}) &= \langle \sin^2 \delta_p \rangle \left[ |P_0|^2 - \frac{1}{2}(|P_+|^2 + |P_-|^2) \right] \\ \sigma \rho_{1-1} &= \frac{1}{2} \langle \sin^2 \delta_p \rangle (|P_+|^2 - |P_-|^2) \end{aligned} \quad (4)$$

$$\begin{aligned} \sigma \text{ Re } \rho_{10} &= \frac{1}{\sqrt{2}} \langle \sin^2 \delta_p \rangle |P_0| |P_-| \xi_{10} \cos \phi_{10} \\ \sigma \text{ Re } \rho_{0s} &= |S_0| |P_0| \xi_{0s} \langle \sin \delta_p \cos(\Delta + \theta_{0s}) \rangle \\ \sigma \text{ Re } \rho_{1s} &= \frac{1}{\sqrt{2}} |S_0| |P_-| \xi_{1s} \langle \sin \delta_p \cos(\Delta + \theta_{1s}) \rangle \end{aligned}$$

where  $\langle \rangle$  indicates an average over the  $K^*$  mass bin. For convenience, we have written the phases,  $\phi_{is}$ , associated with the S-P interference terms [cf. eq.(2)] as  $\phi_{is} = \Delta + \theta_{is}$  where  $\Delta \equiv \delta_s - \delta_p$ .

From eqs. (4) we see that the observables depend only upon the four amplitude magnitudes  $|S_0|$ ,  $|P_0|$ ,  $|P_+|$ ,  $|P_-|$  and the three 'amplitude coherence factors'

$$\begin{aligned}
 C_{10} &\equiv \xi_{10} \cos \phi_{10} \\
 \langle C_{os} \rangle &\equiv \xi_{os} \langle \sin \delta_p \cos(\Delta + \theta_{os}) \rangle \\
 \langle C_{1s} \rangle &\equiv \xi_{1s} \langle \sin \delta_p \cos(\Delta + \theta_{1s}) \rangle
 \end{aligned}
 \tag{5}$$

The  $(P_0, P_-)$  coherence factor satisfies  $|C_{10}| \leq 1$ , whereas the mass-averaged S-P coherences,  $\langle C_{is} \rangle$ , are bounded by  $\pm 0.787$  (see appendix).

### 2.1 Bounds on the $K^*(890)$ amplitudes

From the positivity constraints<sup>6)</sup> on the  $K\pi$  density matrix, we can calculate, using eqs. (4), the range of values allowed for the magnitudes of  $S_0$ ,  $P_0$  and  $P_{\pm}$  and for  $C_{10}$ ,  $\langle C_{1s} \rangle$  and  $\langle C_{os} \rangle$ . The procedure, which includes the averaging over the  $K^*$  mass bin, is outlined in the appendix and the bounds are shown in Fig. 1 in both the  $t$  and  $s$  channel reference frames.

We see that  $P_0$  is by far the largest contribution to the cross section at small  $t$ . This dominance of  $P_0$  can be attributed to the  $\pi$  exchange contribution to the  $t$  channel amplitude  $P_{1+}^0$  (in the notation of eq. (1)). However, by  $-t \sim 0.3 \text{ GeV}^2$ ,  $P_{\pm}$  have magnitudes comparable to that of  $P_0$  and for large  $-t$  ( $\geq 0.4 \text{ GeV}^2$ ),  $P_+$  is the largest amplitude. Moreover,  $P_{\pm}$  do not appear to vanish at  $t' \equiv t - t_{\min} = 0$ . This requires the presence of a contribution which is not (evasive) pole exchange. Such a 'cut' contribution is expected<sup>7,8)</sup> to be present in the  $s$  channel net helicity non-flip amplitudes  $P_{3+}^{\lambda=1}$  and  $P_{1-}^{\lambda=1}$ . It is not possible to disentangle a 'cut' contribution to the other non-flip amplitude,  $P_{1+}^0$ , from the large

$\pi$  exchange contribution. Finally, the bounds on  $C_{10}$  imply that the t-channel  $P_{1+}^-$  amplitude must be non-zero to produce the required coherence of  $P_-$  with the dominant  $\pi$  exchange amplitude.

## 2.2 $K^+p \rightarrow K^*(890)\Delta^{++}$ amplitude analysis

To proceed further we make the reasonable assumption that the dominant  $\pi$  exchange amplitudes are coherent

$$\vec{S}_0 = \gamma_s e^{i\Delta} \vec{P}_0 \quad (6)$$

That is  $\xi_{0s} = 1$  and  $\theta_{0s} = 0$ , which in turn implies  $\xi_{10} = \xi_{1s} \equiv \xi$  and  $\phi_{10} = -\theta_{1s} \equiv \phi$ .

The six observables of eqs. (4) are then given in terms of seven unknowns  $|S_0|$ ,  $|P_0|$ ,  $|P_{\pm}|$ ,  $\xi$ ,  $\phi$  and  $\Delta$ . Apart from the  $(P_0, P_-)$  coherence parameter,  $\xi$ , these equations are identical to those used to analyse the  $\pi^- \pi^+$  angular distribution observed in the reaction  $\pi^- p \rightarrow (\pi^- \pi^+) n$  in the  $\rho$  mass region.<sup>9)</sup> There, the non-evasive contribution to  $P_-$  and the  $\pi$  exchange contribution both occur in s channel baryon flip amplitudes and it is reasonable to assume that  $\xi=1$ . For  $Kp \rightarrow (K\pi)\Delta$  this is not the case and, in fact, from the discussion in the previous section, we expect  $\xi \rightarrow 0$  as  $t' \rightarrow 0$ .

To perform an amplitude decomposition we must therefore make an additional assumption. At the  $\pi$  exchange pole,  $t = \mu^2$ , eq. (6) is exactly true<sup>†</sup>, and  $\Delta$  and  $\gamma_s$  are given in terms of  $K\pi$  phase shifts. However, in the physical region,  $t < t_{\min}$ , modifications can occur. For the amplitude analysis we assume that  $\Delta \equiv \delta_s - \delta_p$  is known and independent of  $t$ , but leave  $\gamma_s$  as a free parameter at each  $t$  value. The value that we use for  $\delta_s$  is that found in the amplitude extrapolation described in §2.3. This value  $\delta_s = 46^\circ$ , which agrees with that obtained<sup>5)</sup> in the amplitude analysis of 13 GeV/c  $K^- p \rightarrow (K^- \pi^+) n$  data<sup>10)</sup> in the same mass region, corresponds to  $\langle C_{0s} \rangle = 0.55$ . With  $\delta_s^3 = -10^\circ$  in eq. (3), this value of  $\delta_s$  implies  $\delta_s^1 = 39^\circ$ .

<sup>†</sup>The amplitudes are also exactly coherent at  $t' = 0$ .

The six remaining unknowns can now be determined from the observables at each value of  $t'$  and the results in the  $t$  channel ( $s$  channel) are shown in Fig. 2a (Fig. 2b). We see that the  $t$  channel ( $s$  channel)  $C_{10}$  and  $\langle C_{1s} \rangle$  are negative (positive) and such that  $\langle C_{1s} \rangle / C_{10} \sim \langle C_{os} \rangle$  which implies that  $\phi \sim 180^\circ (0^\circ)$  and  $\xi \sim -C_{10} (+C_{10})$ . The values found for  $\gamma_s$  can be extrapolated to the  $\pi$  exchange pole. The extrapolated value is in good agreement with that obtained from the  $K\pi$  phases, indicating that the analysis is consistent.

We note that the  $t$  and  $s$  channel amplitudes of Fig. 2a and b, respectively, are obtained under slightly different assumptions and are therefore not exactly related by crossing. The assumption that  $\xi_{os} = 1$  in the  $s$  channel leads to some  $(S_0, P_0)$  incoherence in the  $t$  channel, and vice versa. In practice this difference is negligible except at the largest few  $t$  values considered.

To investigate the sensitivity of the results to the input value of  $\delta_s$ , we repeated the analysis assuming  $\delta_s^1 = 35^\circ$  and  $\delta_s^3 = -10^\circ$  ( $\delta_s = 42^\circ$ ,  $\langle C_{os} \rangle = 0.50$ ). This caused  $\gamma_s$  to increase by about 10% and  $\langle C_{1s} \rangle$  to decrease by about 10%, while the  $P$  wave quantities were virtually unaffected, with the exception of  $|P_+|$  at small  $|t|$ .

From Fig. 2 we see, besides the dominant  $\pi$  exchange in  $P_0$ , the non-evasive contributions to  $P_\pm$ . The coherence,  $|C_{10}|$ , increases rapidly away from  $t'=0$  and we see that  $P_0$  and  $P_-$  are almost coherent<sup>†</sup> for  $0.1 < -t < 0.2 \text{ GeV}^2$ . Another interesting feature is the rapid decrease of  $|P_+|$  to a minimum at  $-t \sim 0.1 \text{ GeV}^2$ , before it increases to exceed  $|P_-|$  and  $|P_0|$  at large  $|t|$ .

---

<sup>†</sup>This is related to the observation in ref. 11 that  $|\text{Re } \rho_{10}|$  for  $K^*_p \rightarrow K^*(890)\Delta^{++}$  reaches its maximum allowed value in this  $t$  interval.

### 2.3 $K^+ p \rightarrow K^*(890)\Delta^{++}$ production mechanisms

We now focus our attention on the question of whether the  $t$  structure of the  $K^+ p \rightarrow K^*(890)\Delta^{++}$  amplitudes can be simply described in terms of production mechanisms expected to be important. For this reaction we have to consider  $\pi$ ,  $B$ ,  $\rho$  and  $A_2$  Regge pole exchanges. We assume  $\pi$ - $B$  and  $A_2$ - $\rho$  exchange degeneracy (EXD) and that the  $\pi$ - $B$  exchange contributes only to the  $t$ -channel non-flip amplitudes,  $S_{1+}^0$  and  $P_{1+}^0$ . This model for the exchanges, along with simple  $t$  channel non-evasive or 'cut' contributions, provides a good description<sup>3)</sup> of 4 GeV/c data<sup>4)</sup> for the line-reversed  $K^+ n \rightarrow K^* p$  and  $K^- p \rightarrow \bar{K}^* n$  reactions, and of the  $K^- p \rightarrow \bar{K}^* n$  data at 13 GeV/c<sup>5)</sup>. For the  $K^+ p \rightarrow K^*(890)\Delta^{++}$  reaction, we find that these simple pole exchanges, together with  $s$  channel non-evasive 'cut' contributions to  $P_{\pm}$ , are a good description of all features of the data. The cuts, when crossed from the  $s$  to the  $t$  channel, automatically generate the observed ( $P_0, P_-$ ) coherence and they also destructively interfere with  $A_2$ - $\rho$  exchange leading to the dip in  $|P_+|$  at  $-t' \sim 0.1 \text{ GeV}^2$ .

We therefore parametrize\* the  $\pi$ - $B$  exchange contribution by

$$(t) P_{1+}^0 = G \frac{K}{\mu^2 - t} \quad (7)$$

where  $K$  is a kinematic factor,<sup>12)</sup>  $K = \left[ (m_{\Delta} + m_N)^2 - t \right] \left[ (m_{\Delta} - m_N)^2 - t \right]^{\frac{1}{2}}$  and  $G = g e^{b(t-\mu^2)}$  is chosen to be real in accord with  $\pi$ - $B$  exchange degeneracy.

The 'cuts' are taken to contribute to the  $s$ -channel net non-flip amplitudes  $P_{3+}^{\lambda=1}$  and  $P_{1-}^{\lambda=1}$  and so we write

$$(s) P_{3+}^1 = G\gamma_3 e^{b_3(t-\mu^2)}$$

$$(s) P_{1-}^1 = G\gamma_1 e^{b_1(t-\mu^2)} \quad (8)$$

\* In the  $t$  dependent analyses, we relate  $t$  to  $t'$  using an effective  $t_{\min}$  of  $-0.014$  and  $-0.051 \text{ GeV}^2$  for the  $K^*(890)$  and  $K^*(1420)$  respectively.

When crossed to the s channel, the  $\pi$ -B exchange of eq. (7) contributes to all the unnatural parity amplitudes and, in conjunction with the cuts of eqs. (8), leads to a  $(P_0, P_-)$  coherence,  $\xi$ , which increases as  $\sqrt{-t'}$  for small  $t'$ .

Motivated by the success of the Stodolsky-Sakurai model<sup>13)</sup> for  $\rho$  exchange, we assume that  $A_2$ - $\rho$  exchange contributes to the t channel amplitudes in the form:

$$\begin{aligned} (t)_{P_{3+}^+} &= \sqrt{3} \quad (t)_{P_{1-}^+} = -t' G\gamma_A e^{b_A(t-\mu^2)} \\ (t)_{P_{3-}^+} &= (t)_{P_{1+}^+} = 0 \end{aligned} \quad (9)$$

where we have taken  $\gamma_A$  to be real, in accord with  $A_2$ - $\rho$  exchange degeneracy. The relative reality of  $\gamma_A$  and the cuts of eqs. (8) is responsible for the dip structure in  $|P_+|$ .

To allow for the S wave under the  $K^*(890)$ , we assume, as in the preceding section, that the (pure  $\pi$ -B exchange)  $S_0$  and  $P_0$  s channel amplitudes are coherent, that is

$$\vec{S}_0 = \gamma_s^\pi e^{b_s(t-\mu^2)} e^{i\Delta} \vec{P}_0 / \cos \chi \quad (10)$$

where  $\chi$  is the crossing angle relating the s and t channel  $K^*$  decay frames. The crossing factor,  $\cos \chi$ , is introduced so that  $\gamma_s^\pi$  is related directly to  $K\pi$  partial waves

$$\gamma_s^\pi = \left| \sin \delta_s^1 e^{i\delta_s^1} + \frac{1}{2} \sin \delta_s^3 e^{i\delta_s^3} \right| / \sqrt{3} \quad (11)$$

This minimal exchange model provides an excellent description of all features of the data. Moreover, as can be seen from the curves on Fig. 2, the t dependence of the amplitudes is in good agreement with the results of

the  $t$ -independent amplitude analysis. The table lists the values of the parameters obtained by fitting to the  $K\pi$  moments (including error correlations) for  $-t' < 0.4 \text{ GeV}^2$ . We note that the non-evasive contributions of eqs. (8) interfere destructively with the  $\pi$ -B pole contributions to these  $s$  channel amplitudes, as would be expected for absorptive corrections to  $\pi$ -B pole exchange.

Since only the  $K\pi$  angular distribution observables are available it is inappropriate to include other possible exchange contributions or to consider refinements to the model. For instance, the P wave amplitudes have been chosen to be relatively real, as required by EXD for  $K^+ p \rightarrow K^* \Delta^{++}$ ; relaxing this constraint and introducing some degree of phase incoherence would not change the essential features of the description, and would only introduce a degree of arbitrariness into the parametrization. However, if the joint  $K^* \Delta^{++}$  decay angular distribution were observed, more detailed features could be explored. For instance, see refs. 2 and 14 where the joint decay distribution is used to study the  $\pi^+ p \rightarrow \rho \Delta^{++}$  ( $\omega \Delta^{++}$ ) amplitudes at 3.7 and 7.1 GeV/c respectively<sup>†</sup>.

### 3. $K^*(1420)$ production

To describe the reaction  $K^+ p \rightarrow (K^+ \pi^-) \Delta^{++}$  in the  $K^*(1420)$  mass region,  $1.36 < M_{K\pi} < 1.48 \text{ GeV}$ , we have to consider S, P and D wave  $K\pi$  spin states. There are therefore nine amplitude vectors<sup>††</sup> ( $S_0, P_0, P_{\pm}, D_0, D_{1\pm}, D_{2\pm}$ ) to determine from the 15 measurable moments of the  $K\pi$  angular distribution ( $\langle Y_M^J \rangle$  with  $J \leq 4, 0 \leq M \leq J$ ).

---

<sup>†</sup>The S wave  $\pi\pi$  contributions under the  $\rho$  have not been studied in these analyses.

<sup>††</sup>The notation is that of §2;  $L_{\lambda\pm}$  describe spin  $L$ , helicity  $\lambda$   $K\pi$  production by natural (+) and unnatural (-) parity exchange.

In principle, we could proceed as we did in the  $K^*(890)$  region and first use the positivity constraints on the  $K\pi$  density matrix to find the allowed range of values of the amplitude magnitudes, and of the coherence factors  $[\text{Re}(\vec{L}_i \cdot \vec{L}_j^*) / |L_i| |L_j|]$  between the various pairs of unnatural (natural) parity exchange amplitudes. Unfortunately, when considering these constraints on the  $K^*(1420)$  amplitudes, it is crucial to include the lower  $K\pi$  partial waves. With S, P and D wave  $K\pi$  production we have to consider 9 magnitudes and 18 coherence factors, and the constraints are very involved and not very illuminating. Given that the P wave under the  $K^*(1420)$  is small, it might appear that we could consider the constraints imposed by the even J moments on the S and D wave  $K\pi$  amplitudes. However, these would be misleading because  $|P_0|^2$  certainly cannot be neglected in comparison to  $|D_{\lambda\pm}|^2$  with  $\lambda=1$  or 2.

### 3.1 $K^+ \rightarrow K^*(1420)\Delta^{++}$ amplitude analysis

In order to determine the  $t$  dependence of the  $K^*(1420)$  production amplitudes, we proceed as we did in the  $K^*(890)$  region. We assume that the dominant  $\pi$  exchange amplitudes are coherent, that is

$$\begin{aligned}\vec{S}_0 &= \gamma_s e^{i\Delta_s} \vec{D}_0 \\ \vec{P}_0 &= \gamma_p e^{i\Delta_p} \vec{D}_0\end{aligned}\tag{12}$$

Since  $\pi$  exchange occurs in the non-flip amplitude component of  $\vec{L}_0$ , these relations are exact at  $t=t_{\min}$  as well as at  $t=\mu^2$ , and should therefore be a good approximation at small  $t'$ .

The relative magnitudes and phases,  $\gamma_s$ ,  $\gamma_p$ ,  $\Delta_s$  and  $\Delta_p$ , at  $t=\mu^2$  can be determined by extrapolation from the physical region  $t' < 0$  to the  $\pi$  exchange pole. Proceeding as we did in the  $K^*(890)$  region, we perform an amplitude analysis at each  $t'$  assuming that  $\Delta_s$  and  $\Delta_p$  are known but

leaving  $\gamma_s$  and  $\gamma_p$  as free parameters. We take  $\Delta_s = 56^\circ$  and  $\Delta_p = 85^\circ$  which are the values found in the amplitude extrapolation described in §3.2.

Before presenting the amplitude analysis it is useful to indicate which moments of the  $K\pi$  angular distribution are primarily responsible for the various amplitude determinations. The even J moments are observed to be much larger than the odd J moments; this requires small P wave  $K\pi$  production under the  $K^*(1420)$ . If, initially, we omit the P wave amplitudes, the even J moments determine  $S_0$ ,  $D_0$ ,  $D_{1\pm}$  and  $D_{2\pm}$ . If, further, we consider only the even J moments with  $M \leq 2$  and neglect  $D_{2\pm}$ , the amplitude determination is very similar to the  $K^*(890)$  analysis. These moments determine  $|S_0|$ ,  $|D_0|$ ,  $|D_{1\pm}|$ ,  $\xi$  and  $\phi$  where

$$\vec{D}_{1-} \cdot \vec{D}_0^* = \xi |D_0| |D_{1-}| e^{i\phi} \quad (13)$$

If we now include the odd J moments and the P wave amplitudes, the moments  $\langle Y_0^1 \rangle$  and  $\langle Y_0^3 \rangle$  are mainly responsible for the determination of  $P_0$  relative to  $S_0$  and  $D_0$ . In practice the amplitude determination is more involved than this simplified discussion implies, since  $|P_0|^2 \approx |D_{1\pm}|^2$  at small  $t$ .

From the above discussion it is clear that we cannot extract the finer details of amplitude structure, such as  $P_{\pm}$ , from the data in the  $K^*(1420)$  mass region. Rather than neglect  $P_{\pm}$  altogether, we include their contributions using the relations

$$\vec{P}_{\pm} = \gamma_p e^{i\Delta_p} \vec{D}_{1\pm} / \sqrt{3} \quad (14)$$

which are expected from absorptive corrections to  $\pi$ -B exchange. We also assume  $D_{2+}$  ( $D_{2-}$ ) is coherent with  $D_{1+}$  ( $D_{1-}$ ). Moreover, we found that leaving the phase  $\phi$ , of eq. (13), free did not significantly improve the description. We therefore set  $\phi=0$  ( $180^\circ$ ) in the s channel (t channel)

amplitude analysis. A reliable determination of  $\phi$  would require even higher statistics data.

The results of the amplitude analysis are shown in Fig. 3. We see that there is a large S wave contribution under the  $K^*(1420)$ . The magnitudes of  $S_0$ ,  $P_0$ ,  $D_0$  and  $D_{1-}$  are reasonably well determined, but we note that  $S_0$  and  $D_0$  are strongly correlated. On the other hand, since the  $(K\pi)$  observables do not contain any interference terms between these amplitudes and  $D_{1+}$ , we find that  $D_{1+}$  is poorly determined at small  $t$ . We note that the  $(D_0, D_{1-})$  coherence,  $\xi$ , has structure very similar to that of  $(P_0, P_-)$  in the  $K^*(890)$  region (cf.  $|C_{10}|$  of Fig. 2). Also non-evasive or 'cut' contributions to  $D_{1\pm}$  are evident from Fig. 3, although  $D_{1+}$  does not appear to exhibit the dip found for  $P_+$  in the  $K^*(890)$  mass region. The variation of the 'cut'/ $\pi$  pole ratio in going from the  $K^*(890)$  to  $K^*(1420)$  mass region is complicated in this reaction by  $t_{\min}$  effects and cannot be immediately deduced from Fig. 3. This variation is studied below.

### 3.2 Production Mechanisms for $K^+p \rightarrow K^*(1420)\Delta^{++}$

As in the  $K^*(890)$  mass region, we determine the structure of the  $K^*(1420)$  amplitudes by fitting directly to the data for  $-t' < 0.3 \text{ GeV}^2$  using an amplitude parametrization based on the production mechanisms. For the D wave amplitudes we use the parametrization of eqs. (7-9) with P replaced by D, with the modification described below. This parametrization leads to non-zero contributions to the  $D_{2\pm}$  amplitudes and, in particular, we find  $\pi$ -B pole contributions to  ${}^{(s)}D_{3+}^{2-}$  and  ${}^{(s)}D_{1-}^{2-}$  which grow as  $(-t')^{\frac{3}{2}}$  and which become too large to agree with the data. This suggests that absorptive corrections should also be included for these amplitudes. Rather than introducing further parameters, we relate these absorptive contributions to those for  ${}^{(s)}D^{\lambda=1}$ , cf eq. (8), using

$$(s)_{D^{\lambda=2}} = \frac{\sqrt{-t'}}{M_{K\pi}} (s)_{D^{\lambda=1}}$$

where the factor  $\sqrt{-t'}/M_{K\pi}$  is expected in an absorbed  $\pi$  exchange picture<sup>15)</sup>.

To allow for the large S wave contribution under the  $K^*(1420)$ , we assume that it is pure  $\pi$ -B exchange and given by (cf. eq. (7))

$$(t)_{S_{1+}^0} = \gamma_s^\pi e^{b_s(t-\mu^2)} e^{i\Delta_s} G \frac{K}{\mu^2-t} \quad (15)$$

The small P-wave contribution, on the other hand, is parametrized by

$$\tilde{P}_0 = \gamma_p e^{i\Delta_p} P \tilde{D}_0 \quad (16)$$

with  $P_\pm$  given by eq. (14).

The values of the parameters listed in the table were obtained by least squares fits to the data in the  $K^*(1420)$  mass region for  $-t' < 0.3 \text{ GeV}^2$ . They provide a good description of the data and the resultant amplitudes compare well with those obtained in the  $t$  independent analysis of §3.1, as can be seen from Fig. 3.

One important result that emerges from the fits is that the  $\pi$ -B exchange contribution to  $K^*(1420)$  production is strongly correlated to that for the large S wave background under the resonance. In particular, although  $\Delta_s$  is well determined, we find a strong correlation between the values of  $G$ ,  $\gamma_s^\pi$  and  $b_s$ . This correlation arises because the extrapolation from the physical region to the  $\pi$  exchange pole is over an interval  $\Delta t \sim 0.07 \text{ GeV}^2$  in the  $K^*(1420)$  region. Equally acceptable descriptions of the data are obtained for values of  $\gamma_s^\pi$  throughout the range  $0.81 < \gamma_s^\pi < 1.10$ , with corresponding ranges for  $G$  and  $b_s$  of  $1.36 > G > 1.14$  and  $1.3 < b_s < 3.3 \text{ GeV}^{-2}$ . These all give very similar descriptions of the  $S_0$  and  $D_0$  amplitudes in the physical region, as indeed they must as these are the best determined amplitudes, but lead to significantly different predictions at the  $\pi$  exchange pole.

It is interesting to see whether the  $M_{K\pi}$  dependence of the  $A_2$ - $\rho$  and cut contributions to  $KN \rightarrow K\pi\Delta$  is similar to that found in the  $KN \rightarrow K\pi N$  reactions. From the table, we see that the ratio of  $A_2$ - $\rho$  to  $\pi$ -B exchange at  $-t=0.3 \text{ GeV}^2$  is only half as large in the  $K^*(1420)\Delta$  region as it is for  $K^*(890)\Delta$ . This mass dependence agrees well with that found in the  $\bar{K}^*n$  reactions<sup>5)</sup>, although the size of the  $A_2$ - $\rho$  coupling is not very well determined in the  $K^*(1420)$  region in either case.

In order to compare the strength of the 'cuts' in the  $K^*(890)$  and  $K^*(1420)$  regions it is useful to compare them with the expectations of the Williams model<sup>7)</sup>. That is, in the s-channel evasive amplitudes,  $L_{3+}^{\lambda=1}$  and  $L_{1-}^{\lambda=1}$  we make the replacement

$$\frac{t'}{\mu^2-t} \rightarrow \frac{t'}{\mu^2-t} + C_W \quad (17)$$

where  $C_W$  may be regarded as an absorptive correction to the  $\pi$  exchange contribution  $t'/\mu^2-t$ . The Williams model takes  $C_W=1$ . In the  $K^*(890)$  region, we find at  $-t=.056 \text{ GeV}^2$  that  $C_W=1.0$  in  $P_{3+}^1$  and  $C_W=1.9$  in  $P_{1-}^1$ . In the  $K^*(1420)$  region, we find  $C_W=0.4$  (0.7) in  $D_{3+}^1$  ( $D_{1-}^1$ ) at the same  $t$  value. These numbers are very similar to those found for the  $KN \rightarrow K^*N$  reactions, namely  $C_W=1.1$  (0.6) in the  $K^*(890)$  ( $K^*(1420)$ ) regions. That is, in  $K\pi\Delta$  production, as well as in the  $K\pi n$  and  $\pi\pi n$  reactions<sup>5,15,16)</sup> there is a marked decrease of the 'cut' effect with increasing meson mass.

#### 4. Summary and Conclusions

We have studied the structure of the  $K^*(890)$  and  $K^*(1420)$  production amplitudes using the moments of the  $K\pi$  angular distribution observed in the reaction  $K^+ p \rightarrow K^+ \pi^- \Delta^{++}$  at 13 GeV/c. Although it might appear that such an analysis can only be performed if the joint  $K^*\Delta$  decay distribution is available, we have shown that, for this  $\pi$  exchange dominated reaction, a reasonable amplitude determination can be achieved even when the  $\Delta$  decay is not observed.

For the determination of  $K^*$  production amplitudes we found that it is crucial to include amplitudes describing the production of the lower  $K\pi$  spin states. In the  $K^*(890)$  mass region this is illustrated by the amplitude bounds (Fig. 1) which follow directly from the positivity of the density matrix. Whereas  $|P_0|$  is well-determined by the data, we see that  $|P_{\pm}|$  and the coherence factors are sensitive to the S wave under the  $K^*(890)$ . Moreover in the  $K^*(1420)$  region we found that the S and P wave amplitudes,  $S_0$  and  $P_0$ , are at least as important as those describing non-zero helicity  $K^*(1420)$  production (namely  $D_{1\pm}$  and  $D_{2\pm}$ ).

We summarize our results on the  $K^*(890)$  and  $K^*(1420)$  amplitude structure and production mechanisms with reference to Figs. 2 and 3. In the forward direction we see that the  $K^*$  resonances are produced dominantly in the helicity zero state, as expected from the presence of the nearby  $\pi$  exchange pole. This implies that the  $K^+_p \rightarrow K^*\Delta^{++}$  helicity amplitude,  $L_{1+}^0$ , dominates near  $t'=0$ . We also see evidence for non-evasive helicity one  $K^*$  production, which implies the presence of production amplitudes  $L_{3+}^1$  and/or  $L_{1-}^1$  at  $t'=0$ . In addition we see that the  $(L_{1-}, L_0)$  coherence increases rapidly from zero at  $t'=0$  such that  $L_0$  and  $L_{1-}$  have a large degree of coherence by  $-t' \sim 0.1 \text{ GeV}^2$ . We find that  $\pi$  exchange and s channel non-evasive contributions give a natural explanation of the observed  $t$  structure of the coherence. Furthermore the dip at  $-t' \sim 0.1 \text{ GeV}^2$  in the natural parity exchange contribution can be described by destructive interference between  $A_2$ - $\rho$  exchange and these non-evasive contributions. The natural parity exchange amplitude,  $D_{1+}$ , describing  $K^*(1420)$  production does not show this structure, although it is less well determined due, to a large extent, to appreciable S and P wave  $K\pi$  production in the  $K^*(1420)$  mass region. These lower partial wave amplitudes are, respectively, some 90% and 20% of the helicity zero  $K^*(1420)$  production amplitude,  $D_0$ .

A comparison of the  $K^*(890)$  and  $K^*(1420)$  amplitudes allows a study of the  $K\pi$  mass dependence of the exchange mechanisms for  $K^+p \rightarrow (K\pi)\Delta^{++}$ . As for  $Kp \rightarrow (K\pi)n$  and  $\pi p \rightarrow (\pi\pi)n$ , we find that the absorptive corrections (and also  $A_2$ - $\rho$  exchange) decrease relative to  $\pi$  exchange with increasing mass.

Finally, we compare the  $K\pi$  partial waves found in the  $K^*$  resonance regions by analysing  $K^+p \rightarrow (K\pi)\Delta^{++}$  data, with those obtained<sup>5)</sup> using 13 GeV/c  $K^-p \rightarrow (K\pi)n$  data<sup>10)</sup>. The results, obtained by extrapolating the  $\pi$  exchange amplitude contributions to  $t=\mu^2$ , are in reasonable agreement (compare the values of  $\delta_s^1$ ;  $\gamma_s^\pi$ ,  $\Delta_s$ ,  $\gamma_p$  and  $\Delta_p$  in the table with those of ref. 5). As compared to  $Kp \rightarrow (K\pi)n$ , the reaction  $Kp \rightarrow (K\pi)\Delta$  has the advantage that  $\pi$  exchange occurs in non-flip amplitudes. However, in the  $K^*(1420)$  mass region we find that the  $K\pi$  partial waves are better-determined using  $K^-p \rightarrow (K\pi)n$  data. The advantage of the non-flip  $\pi$  exchange contributions to  $Kp \rightarrow (K\pi)\Delta$  is more than offset by the larger value of  $t_{\min}$  ( $t_{\min} = -0.051 \text{ GeV}^2$  for  $K^+p \rightarrow K^*(1420)\Delta^{++}$  at 13 GeV/c) which gives rise to a much larger extrapolation interval than for  $K^-p \rightarrow K^*(1420)n$ .

Positivity<sup>6)</sup> imposes constraints on the  $K\pi$  density matrix elements or, alternatively, bounds on the amplitude magnitudes,  $|L_\lambda|$ , and the coherence factors,  $C_{ij}$ ; defined in eqs. (5). In principle, the problem can be separated into two parts, that is, the natural and unnatural parity exchange parts of the density matrix are block diagonal. However, in the case of a superposition of two (or more) spin states, the data do not permit such a separation into natural and unnatural parity sectors. Furthermore, in the  $K^*(890)$  mass region, the problem is complicated by the fact that the P wave amplitudes are rapidly varying functions of  $K\pi$  mass while the S wave is virtually independent of  $M_{K\pi}$ . In eqs. (4) and (5) this  $M_{K\pi}$  dependence is explicitly exhibited.

Before considering the positivity constraints we note that, because of the mass averaging, the S-P coherences  $\langle C_{os} \rangle$  and  $\langle C_{1s} \rangle$  are unlike  $C_{10}$ , not bounded by  $\pm 1$ . To see this we write, for instance,  $\langle C_{os} \rangle$  of eq. (5) as

$$\begin{aligned} \langle C_{os} \rangle &= \xi_{os} \langle \sin \delta_p \cos(\delta_s - \delta_p + \theta_{os}) \rangle \\ &\equiv a \xi_{os} \cos \bar{\theta} \equiv a C_{os} \end{aligned}$$

where  $a$  is given by

$$a = \left[ \langle \sin^2 \delta_p \rangle^2 + \langle \sin \delta_p \cos \delta_p \rangle^2 \right]^{\frac{1}{2}} = 0.787$$

and, analogously,  $\langle C_{1s} \rangle = a C_{1s}$ . The positivity constraints apply to the matrix constructed from the  $|L_\lambda|$  and these  $C_{ij}$ , which satisfy  $|C_{ij}| \leq 1$ .

It is convenient to discuss the bounds in three stages. First we have the bounds on the amplitude magnitudes, that is,  $|L_\lambda|^2 \geq 0$ , where  $L_\lambda = S_0, P_0, P_-$  or  $P_+$ . From the first three of eqs.(4), we can express  $|S_0|^2$ ,  $|P_+|^2$  and  $|P_-|^2$  in terms of, say,  $|P_0|^2$  and the observables. The

magnitude bounds for  $P_+$ ,  $P_-$  and  $P_0$  all provide lower bounds on  $|P_0|$  while the bound on  $|S_0|$  gives an upper bound on  $|P_0|$ . In the small  $t'$  region ( $-t' < .12 \text{ GeV}^2$ ), we find that the lower bound for  $|P_0|$  generally corresponds to  $|P_+|=0$ .

The second type of bound comes from the Schwarz inequalities for the unnatural parity amplitudes, that is  $\text{Re}(\vec{L}_i \cdot \vec{L}_j^*) \leq |L_i| \cdot |L_j|$ , or  $|C_{ij}| \leq 1$ . By using eqs. (4), we can express the  $C_{ij}$  in terms of observables and  $|P_0|^2$ . The bound on  $C_{10}$  yields a lower bound for  $|P_0|$  while those for  $C_{os}$  and  $C_{1s}$  give both upper and lower limits. For  $-t' > .12 \text{ GeV}^2$ , we find that  $|C_{10}| \leq 1$  provides the tightest lower bound on  $|P_0|$  while for virtually the entire  $t$  range the best upper bound comes from  $|C_{os}| \leq 1$ .

The third category of bound comes from the requirement that the determinant of the unnatural parity sector of the density matrix be positive. In terms of the  $C_{ij}$ , this can be written as

$$C_{10}^2 + C_{os}^2 + C_{1s}^2 - 2 C_{os} C_{1s} C_{10} \leq 1$$

which can be easily derived using the cosine addition theorem. After expressing the  $C_{ij}$ 's in terms of  $|P_0|^2$  and the observables, this becomes a cubic in  $|P_0|^2$ , and, in practice, generates an upper and a lower bound on  $|P_0|^2$ . We find that, in general, these bounds are slightly more restrictive than those of the first two categories.

References

- 1) G. W. Brandenburg et al, SLAC report (in preparation)
- 2) A. C. Irving, Nucl. Phys. B63 (1973) 499
- 3) P. Estabrooks and A. D. Martin, Nucl. Phys. B102 (1976) 537
- 4) A. B. Wicklund et al, ANL report (in preparation)
- 5) P. Estabrooks et al, SLAC-PUB-1701 (1976)
- 6) S. U. Chung and T. L. Trueman, Phys. Rev. D11 (1975) 633
- 7) P. K. Williams, Phys. Rev. D1 (1970) 1312
- 8) M. Ross, F. S. Henyey and G. L. Kane, Nucl. Phys. 23B (1970) 269
- 9) P. Estabrooks and A. D. Martin, Phys. Letters 41B (1972) 350
- 10) G. W. Brandenburg et al, Phys. Letts. 59B (1975) 405
- 11) G. Ciapetti et al, Nucl. Phys. B64 (1973) 58
- 12) S. Frautschi and L Jones, Phys. Rev. 164 (1967) 1918
- 13) L. Stodolsky and J. J. Sakurai, Phys. Rev. Letters 11 (1963) 90
- 14) J. F. Owens, R. L. Eisner, S. U. Chung and S. D. Protopopescu,  
Phys. Letts. 58B (1975) 376
- 15) A. D. Martin, Proc. of the IV International Symposium on  
Multiparticle Hadrodynamics, Pavia, eds. F. Duimio, A. Giovannini  
and S. Ratti (1973) 203
- 16) W. Ochs and F. Wagner, Phys. Letts. 44B (1973) 271

TABLE

The values of the parameters obtained by fitting to  $K^+p \rightarrow K^+\pi^-\Delta^{++}$  data in the  $K^*(890)$  and  $K^*(1420)$  mass regions using the parametrizations described in §2.3 and §3.2 respectively.

	$K^*(890)$	$K^*(1420)$
$g$	1.43	1.26
$b$	-1.2	0.2
$\gamma_3$	-5.5	-3.0
$b_3$	-1.1	-1.9
$\gamma_1$	-9.5	-5.1 <sup>a)</sup>
$b_1$	1.4	0.6
$\gamma_A$	57	6.3
$b_A$	4.4	-
Parameters describing the lower $K\pi$ waves	$\delta_s^1 = 39^\circ$ $b_s = 6.4$	$\gamma_s^\pi = 1.03$ $\Delta_s = 56^\circ$ $b_s = 2.3$ $\gamma_p = 0.21$ $\Delta_p = 86^\circ$

a) In the  $K^*(1420)$  fits we have imposed the constraint that  $\gamma_1/\gamma_3$  equal its value in the  $K^*(890)$  fits.

Figure Captions

- Fig. 1 The bounds for the  $K^+p \rightarrow K\pi\Delta^{++}$  amplitudes in the  $K^*(890)$  mass region, obtained from the positivity of the  $K\pi$  density matrix. The quantities are defined by eqs. (4) and (5), and  $\gamma_s = |S_0|/|P_0|$ . The S-P coherence factors are averaged over the  $K^*$  mass bin and are therefore bounded by  $\pm 0.787$  (see the appendix). Figs. a) and b) correspond to using the t and s channel frames to describe the  $K\pi$  angular distribution. The bounds on  $|P_+|$  are the same in both channels.
- Fig. 2 The 13 GeV/c  $K^+p \rightarrow (K\pi)\Delta^{++}$  amplitudes obtained by analysing the  $K\pi$  angular distribution in the  $K^*(890)$  mass region. The points are the results of the amplitude analysis described in §2.2, and the curves correspond to the fit, described in §2.3, to data with  $-t' < 0.4 \text{ GeV}^2$ .
- Fig. 3 The 13 GeV/c  $K^+p \rightarrow (K\pi)\Delta^{++}$  amplitudes obtained by analysing the  $K\pi$  angular distribution in the  $K^*(1420)$  mass region. The points are the results of the amplitude analysis described in §3.1, and the curves correspond to the fit, described in §3.2, to data with  $-t' < 0.3 \text{ GeV}^2$ .

BOUNDS FOR  $K^+ p \rightarrow K^*(890) \Delta^{++}$  AMPLITUDES AT 13 GeV/c

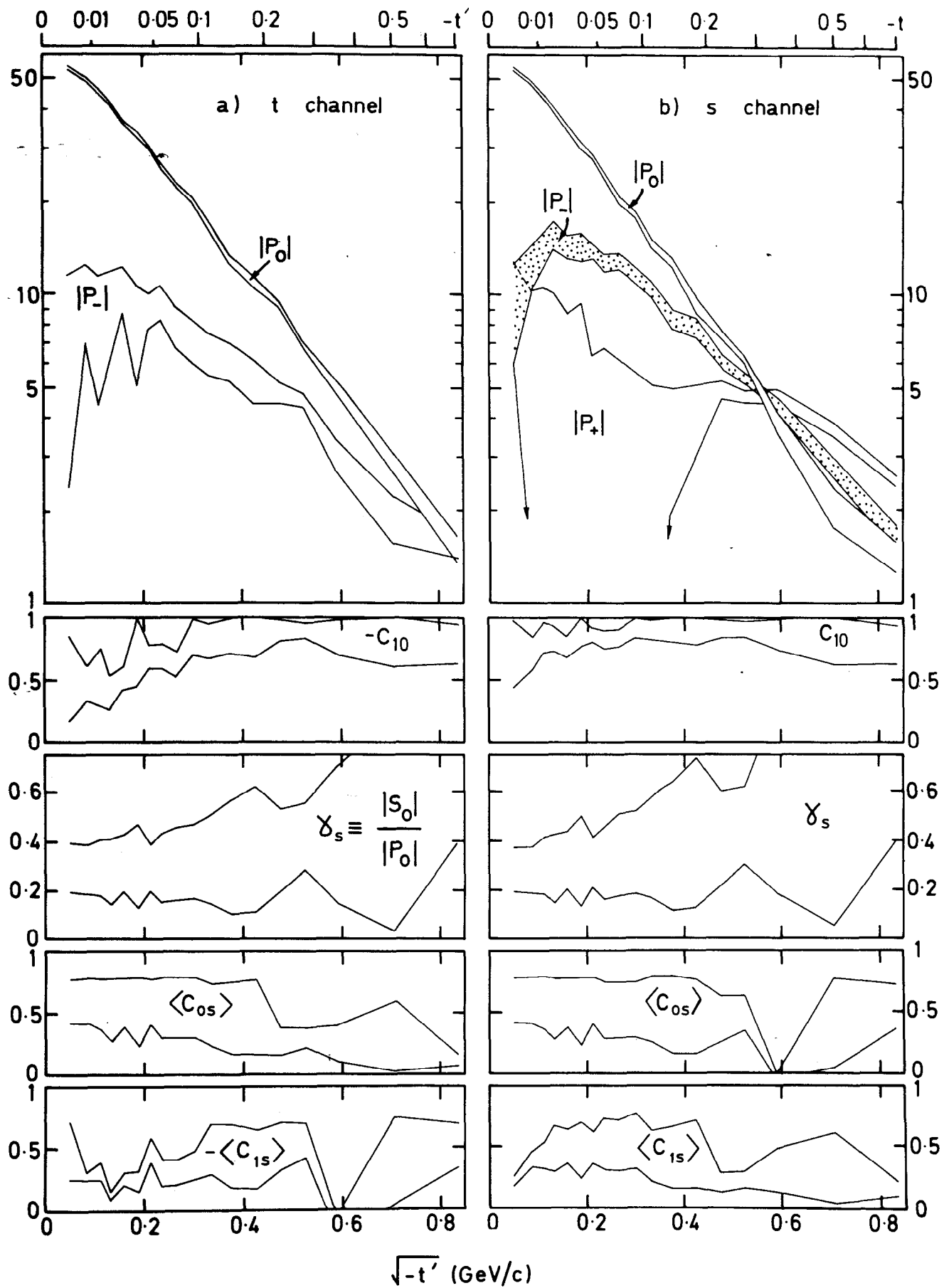


FIG. 1

$K^+ p \rightarrow K^* (890) \Delta^{++}$  AMPLITUDES AT 13 GeV/c

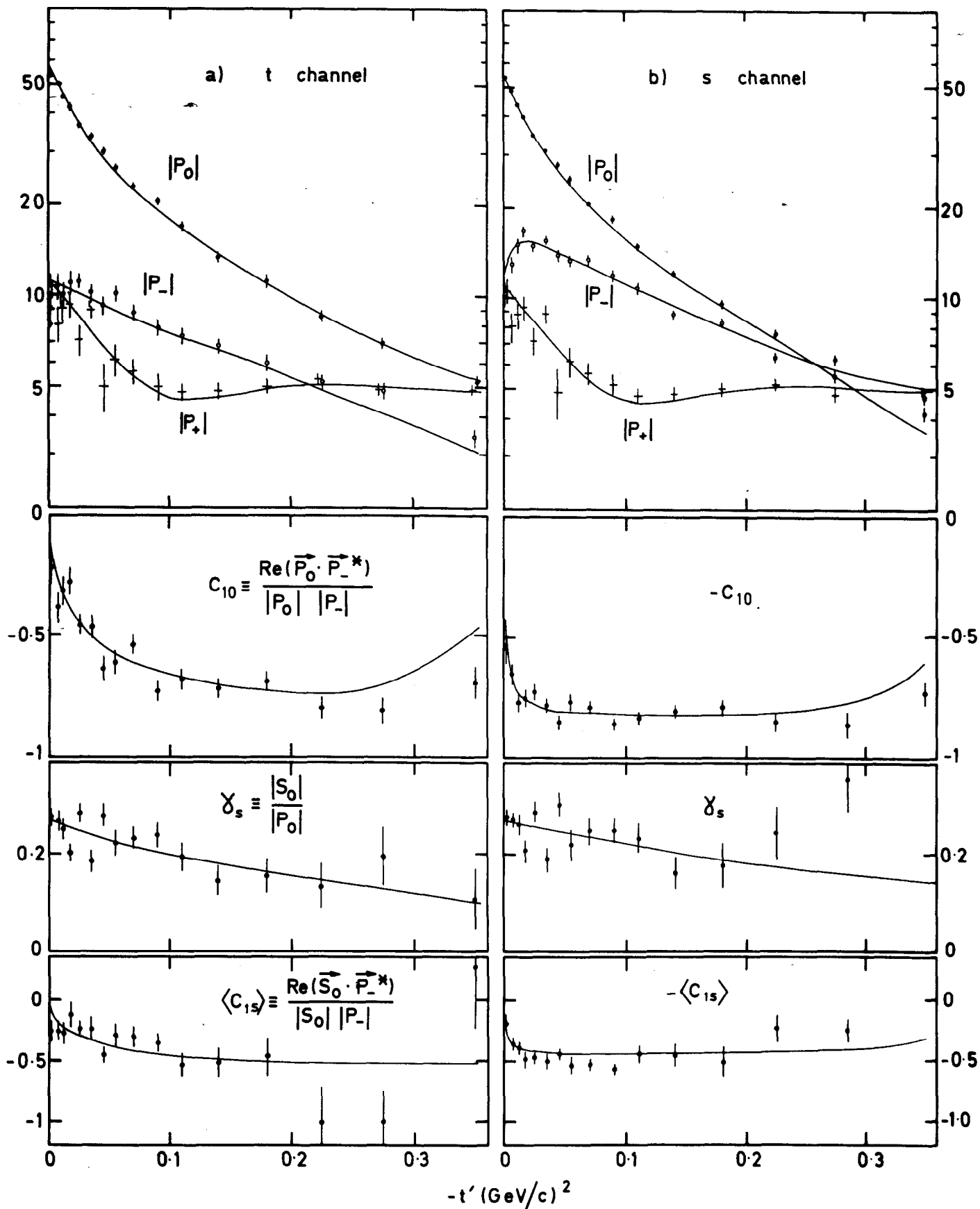


FIG. 2

# $K^+ p \rightarrow K^*(1420) \Delta^{++}$ AMPLITUDES AT 13 GeV/c

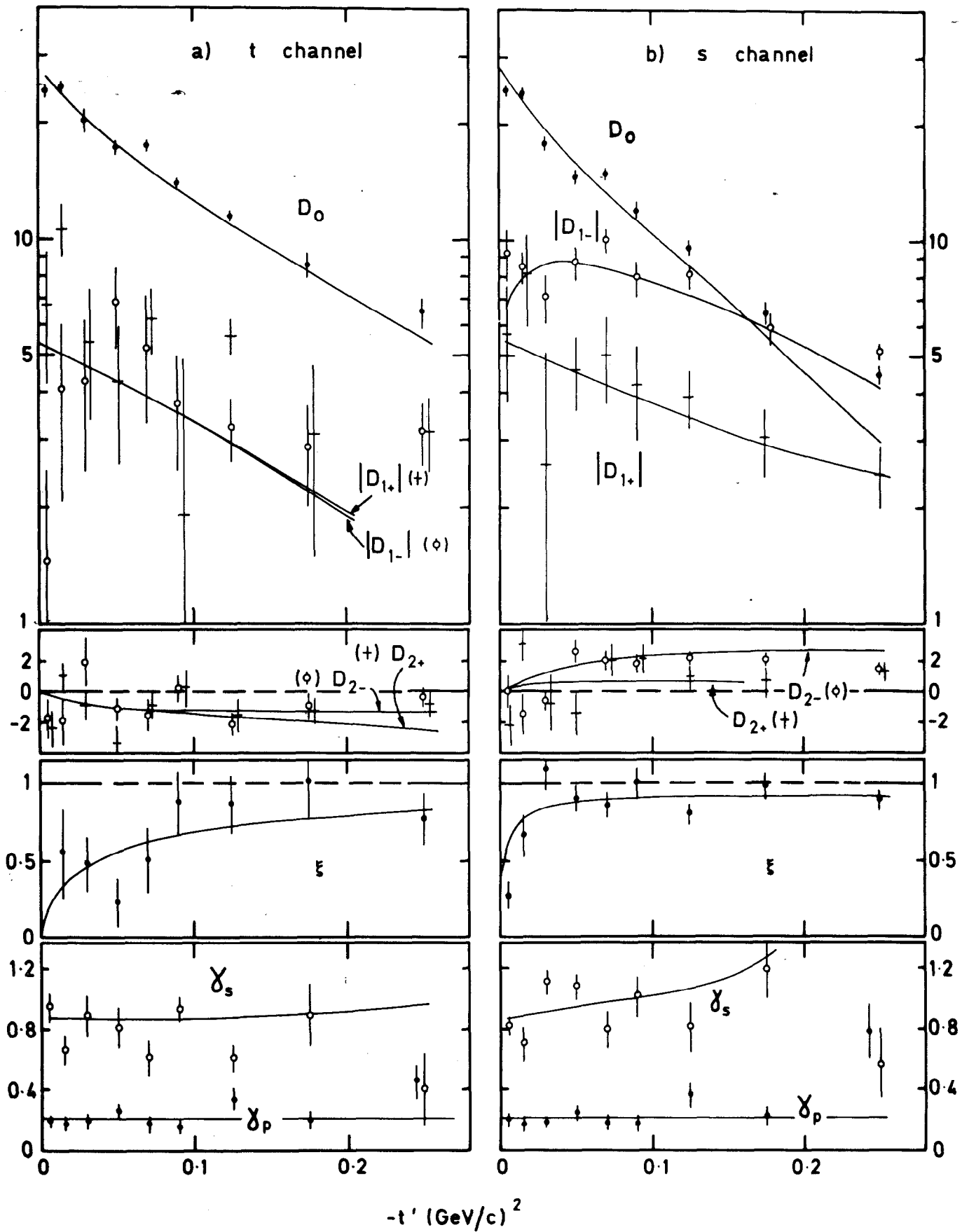


FIG. 3